PHYSICAL REVIEW B VOLUME 32, NUMBER 10 15 NOVEMBER 1985

Bulk and surface plasmons and localization effects in finite superlattices

B. L. Johnson
Department of Physics, University of Colorado, Colorado Springs, Colorado 80933-7150

Jerome T. Weiler
Department of Mathematics, University of Colorado, Colorado Springs, Colorado 80933-7150

R. E. Camley
Department of Physics, University of Colorado, Colorado Springs, Colorado 80933-7150
(Received 2 May 1985)

We consider the propagation of bulk and surface plasmons in a finite superlattice structure composed of alternating layers of materials A and B, with the whole structure resting on a substrate. An implicit dispersion relation is derived allowing the dielectric constant of each material to be a function of frequency. We then present numerical examples for the case where material A is a metal and the remaining materials have frequency-independent dielectric constants. We explore three types of material configurations: (1) a finite number of layers of A and all other materials being taken with $\epsilon=1$; (2) the same as case (1), but here with the dielectric constant of material B increased by 5%; and (3) a realistic geometry appropriate for Al films separated by Al_2O_3 layers on a SiO_2 substrate. The dispersion curves in case (1) are similar to those for an infinite superlattice of the same material parameters. The primary difference is that for thin superlattice structures, there is a splitting of the frequencies of the surface modes. In case (2) the symmetry of the system is lowered and there is strong localization, particularly for the surface modes. Case (3) also shows unique features, the most interesting being the existence of a mode which changes character from bulk nature to a surface mode and then back to a bulk mode.

I. INTRODUCTION

There has been considerable interest recently in the properties of superlattices. Initial investigations have been made of the properties of various types of collective excitations of the superlattices, such as magnons,[1-6] phonons,[7-14] and plasmons.[15-22] It has been found that these excitations exhibit properties unique to the superlattice structure. For example, the existence of a surface wave on a semi-infinite superlattice can depend critically on the ratio of the thicknesses of the two alternating materials.

In this paper we will look closely at some of the properties of bulk and surface plasmons in finite superlattices. We note that bulk plasmons in superlattices have already been observed in GaAs-(AlGa)As by inelastic light scattering.[20] There has also been a reasonable amount of theoretical development in understanding the properties of plasmons in superlattices.[15-19,21,22]

One can understand the collective excitation of a superlattice plasmon in the following way. An excitation of a surface plasmon in one material layer produces electric fields outside its boundaries. These fields in turn couple with the elementary excitations of the other layers. By invoking Bloch's theorem, one sees that this coupling creates a set of collective excitations of the entire superlattice. This set of excitations is characterized by a wave vector normal to the material interfaces as well as a wave vector parallel to the interfaces. Previous theoretical studies have shown that if one plots a dispersion curve of frequency versus the wave vector parallel to the interfaces, one sees bands where bulk superlattice plasmons exist. If we represent the wave vector perpendicular to the interfaces by $q_\perp$, and the unit-cell length of the superlattice by L, the boundaries of the bulk bands exist when $q_\perp L=0$ or π. In the gaps between the bulk bands, and above and below the bands, one can find the surface waves.

Previous theoretical work on plasmons in superlattices have concentrated on geometries which were infinite or semi-infinite. In this paper we concentrate on a finite-superlattice structure on a substrate. We note that the properties of magnons in a finite superlattice have been investigated.[3] The method used here provides a simpler answer and more physical insight than the method used in studying finite magnetic superlattices. This geometry represents a physically realizable case. Also, as we shall see, the plasmon dispersion curves have unique features due to the finite thickness. Thus in this paper we want to discuss two questions:

(1) How many layers are necessary before a superlattice can be adequately modeled by a semi-infinite or infinite structure?

(2) Are there any features of the finite structure which do not exist in the semi-infinite structure?

We will see that the finite structure does have some very interesting results. In particular, we will see that small changes in the wave vector parallel to the surface of the superlattice can lead to dramatic changes in the localization of the excitation. Similarly, small changes in the

properties of the constituent materials of the superlattice can also lead to significant localization of the plasmon.

The remainder of this paper is organized as follows. In Sec. II we present a brief review of the methods and results used to find dispersion curves for semi-infinite superlattices, and then summarize the results for that structure. An implicit dispersion relation is then derived for the finite superlattice on a substrate. In Sec. III we present numerical studies of the dispersion-relation results for particular material parameters. In Sec. IV we explore the spatial distribution of the superlattice excitations and show how localization can result from small changes. Finally, in Sec. V we summarize our results.

II. THEORY

In this section we present the development of the general dispersion relations for bulk and surface plasmons on a finite superlattice. We begin, however, with a brief review of the method used in an infinite superlattice.

We consider a superlattice composed of alternating layers of material A and B, with dielectric constants $\epsilon_A(\omega)$ and $\epsilon_B(\omega)$, respectively. Material A always has a thickness d_1 and material B always has a thickness d_2. To find the dispersion relation for bulk and surface plasmons, we begin by noting that the electrostatic potential $\phi(\mathbf{x},t)$ must satisfy Laplace's equation

$$\nabla^2\phi(\mathbf{x},t)=0 \tag{1}$$

in all regions. In addition, this potential must satisfy boundary conditions at each material A-B interface. These boundary conditions state that the electrostatic potential must be continuous, and the normal component of the displacement must be continuous, at each interface.

We establish the coordinates with the z axis normal to each A-B interface, and the x axis parallel to the same. Since we have translational invariance in the x and y directions, the wave vector $\mathbf{k}$ is completely characterized by x and z. The electrostatic potential will have the form

$$\phi(x,y,z,t)=\Phi(z)e^{i(kx-\omega t)} , \tag{2}$$

and applying Eq. (1) yields

$$\left[\frac{d^2}{dz^2}-k^2\right]\Phi(z)=0 \tag{3}$$

with the general solution

$$\Phi(z)=A_+e^{+kz}+A_-e^{-kz} . \tag{4}$$

Since the structure is periodic, we invoke Bloch's theorem, and look for solutions of the form

$$\Phi(z)=e^{iqz}U_q(z) , \tag{5}$$

where for any integer n, and $L=d_1+d_2$,

$$U_q(z+nL)=U_q(z) . \tag{6}$$

One finds that the most general solution which satisfies both Eqs. (3) and (6) is

$$U_q(z)=e^{-iq(z-nL)}(A_+e^{k(z-nL)}+A_-e^{-k(z-nL)}) , \quad nL\le z\le nL+d_1 \tag{7}$$

for material A, and a similar result for material B. Note that q is a wave vector that will arise in the dispersion relation for the collective excitations. Upon applying Eq. (7) to (5), we arrive at the electrostatic potential for material A,

$$\Phi(z)=e^{iqnL}(A_+e^{k(z-nL)}+A_-e^{-k(z-nL)}) , \quad nL\le z\le nL+d_1 . \tag{8}$$

In a similar manner, we arrive at the electrostatic potential in material B,

$$\Phi(z)=e^{iqnL}(B_+e^{k(z-nL-d_1)}+B_-e^{-k(z-nL-d_1)} , \quad nL+d_1\le z\le(n+1)L . \tag{9}$$

To solve for the arbitrary constants A_+, A_-, B_+, and B_-, we invoke the boundary conditions previously described to yield the following four equations:

$$A_+e^{kd_1}+A_-e^{-kd_1}=B_++B_- , \tag{10}$$

$$\epsilon_A(\omega)(A_+e^{kd_1}-A_1e^{-kd_1})=\epsilon_B(\omega)(B_+-B_-) , \tag{11}$$

$$A_++A_-=e^{-iqL}(B_+e^{kd_2}+B_-e^{-kd_2}) , \tag{12}$$

$$\epsilon_A(\omega)(A_++A_-)=\epsilon_B(\omega)e^{-iqL}(B_+e^{kd_2}-B_-e^{-kd_2}) . \tag{13}$$

The result of translating these equations into matrix form and setting the determinant of the coefficient matrix equal to zero is an implicit dispersion relation,

$$\left[1+\left[\frac{\epsilon_A(\omega)}{\epsilon_B(\omega)}\right]^2\right]\sinh(kd_2)\sinh(kd_1) +2\frac{\epsilon_A(\omega)}{\epsilon_B(\omega)}[\cosh(kd_2)\cosh(kd_1)-\cos(qL)]=0 . \tag{14}$$

The above dispersion relation will be assumed to hold in

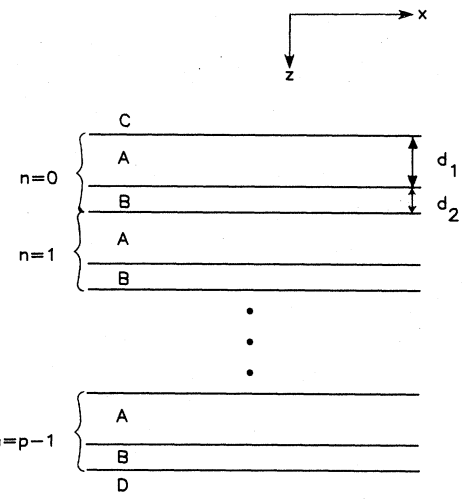

FIG. 1. Superlattice of finite extent. The structure is composed of alternating layers of materials A and B, the spaces above and below the structure are filled with materials C and D, respectively, and each material is characterized by the appropriate dielectric constant. The unit cells are indexed by n, as shown.

the interior of the finite superlattice.

We now turn to the determination of the dispersion relation for finite superlattices. The structure is illustrated in Fig. 1. The finite superlattice has a total of p unit cells, where a unit cell is composed of one film of material A and one of material B. We assume that the superlattice rests on a substrate of material D with dielectric constant $\epsilon_D(\omega)$, and above the structure is material C with dielectric constant $\epsilon_C(\omega)$.

We now discuss the form of the solution for the finite superlattice. First we note that for the infinite superlattice the solution for the electrostatic potential was essentially composed of a surface-wave electrostatic potential in each film multiplied by an envelope function (the e^{iqnL} term) which related the amplitudes of one film to another. For the finite-superlattice problem we must have a sum of two such terms in the interior of the superlattice, where each term has a different envelope function. If one discusses surface waves, the envelope functions should have the forms $e^{-\gamma nL}$ and $e^{-\gamma(p-n)L}$. These forms correspond to envelope functions which are localized at the top and bottom surface of the superlattice, respectively. For bulk waves in the superlattice one replaces γ with $-iq$. This brings us back to forms similar to those in Eqs. (8) and (9). We therefore take the following as the form of the electrostatic potential:

$$\Phi(z)=Ce^{kz} \text{ for } z\le 0,$$

$$\Phi(z)=e^{-\gamma nL}(A_+e^{k(z-nL)}+A_-e^{-k(z-nL)})+e^{-\gamma(p-n)L}(A_+e^{k(z-nL)}+A_-e^{-k(z-nL)}) \text{ for } nL\le z\le nL+d_1 ,$$

$$\Phi(z)=e^{-\gamma nL}(B_+e^{k(z-nL-d_1)}+B_-e^{-k(z-nL-d_1)})+e^{-\gamma(p-n)L}(B_+e^{k(z-nL-d_1)}+B_-e^{-k(z-nL-d_1)}) \text{ for } nL+d_1\le z\le (n+1)L, \tag{15}$$

$$\Phi(z)=De^{-k(z-pL)} \text{ for } z\ge pL .$$

It is clear that if we incorporate $e^{-\gamma pL}$ into A_+, A_-, B_+, and B_- to obtain new coefficients A'_+, A'_-, B'_+, and B'_-, we can rewrite Eq. (15) as follows:

$$\Phi(z)=Ce^{kz} \text{ for } z\ge 0,$$

$$\Phi(z)=e^{-\gamma nL}(A_+e^{k(z-nL)}+A_-e^{-k(z-nL)})+e^{\gamma nL}(A'_+e^{k(z-nL)}+A'_-e^{-k(z-nL)}) \text{ for } nL\le z\le nL+d_1,$$

$$\Phi(z)=e^{-\gamma nL}(B_+e^{k(z-nL-d_1)}+B_-e^{-k(z-nL-d_1)})+e^{\gamma nL}(B'_+e^{k(z-nL-d_1)}+B'_-e^{-k(z-nL-d_1)}) \text{ for } nL+d_1\le z\le (n+1)L, \tag{16}$$

$$\Phi(z)=De^{-kz} \text{ for } z\ge pL .$$

We will solve for the coefficients as follows.

(i) We will assume that $e^{-\gamma nL}$ is an envelope function which is associated with a traveling wave propagating down the stack from $z=pL$. (Note that if γ is real and positive, the envelope function is that of an exponentially decaying wave localized at the top surface.) This assumption allows us to relate A_+ and A_- to B_+ and B_- and, independently, we can relate A'_+ and A'_- to the B'_+ and B'_- for the wave with the $e^{+\gamma nL}$ envelope. Ultimately, we will relate the A_+ to the A_-, and then the A'_+ to the A'_-, leaving A_+ and A'_+ as the only unknowns.

(ii) We will then impose the boundary conditions at $z=0$, the C-A interface, and at $z=pL$, the B-D interface. The result will be four homogeneous linear equations in four unknowns, A_+, A'_+, C, and D. These will yield a solution only if the determinant of the coefficient matrix vanishes.

We first deal with the interior boundary conditions. We impose the requirement of continuity of Φ and continuity of the displacement, $\mathbf{D}$, which is equivalent to requiring continuity of $\epsilon(\omega)[\partial\Phi(z)/\partial z]$ at each A-B and B-A interface. Consider the wave with the $e^{-\gamma nL}$ envelope function. At $z=nL+d_1$, an A-B interface, continuity of Φ gives us

$$A_+e^{kd_1}+A_-e^{-kd_1}=B_++B_- . \tag{17}$$

Continuity of $\epsilon_A(\omega)[\partial\Phi(z)/\partial z]$ gives us

$$\epsilon_A(\omega)(A_+e^{kd_1}-A_1e^{-kd_1})=\epsilon_B(\omega)(B_+-B_-) . \tag{18}$$

Similarly, at the B-A interface, $z=nL+d_1$, we obtain

$$A_++A_-=e^{\gamma L}(B_+e^{kd_2}+B_-e^{-kd_2}) \tag{19}$$

and

$$\epsilon_A(\omega)(A_+-A_-)=\epsilon_B(\omega)e^{\gamma L}(B_+e^{kd_2}-B_-e^{-kd_2}) . \tag{20}$$

In exactly the same fashion, we obtain for the traveling wave associated with the envelope function $e^{\gamma nL}$ the following at the A-B interface:

$$A'_+e^{kd_1}+A'_-e^{-kd_1}=B'_++B'_- , \tag{21}$$

$$\epsilon_A(\omega)(A'_+e^{kd_1}-A'_-e^{-kd_1})=\epsilon_B(\omega)(B'_+-B'_-) , \tag{22}$$

and for the B-A interface,

$$A'_++A'_-=e^{-\gamma L}(B'_+e^{kd_2}+B'_-e^{-kd_2}) , \tag{23}$$

$$\epsilon_A(\omega)(A'_+-A'_-)=\epsilon_B(\omega)e^{-\gamma L}(B'_+e^{kd_2}-B'_-e^{-kd_2}) . \tag{24}$$

Next, we solve for B_+, B_-, B'_+, and B'_- as follows:

$$B_+=\frac{1}{2}\left[A_+e^{kd_1}\left[1+\frac{\epsilon_A}{\epsilon_B}\right]+A_-e^{-kd_1}\left[1-\frac{\epsilon_A}{\epsilon_B}\right]\right], \tag{25}$$

$$B_-=\frac{1}{2}\left[A_+e^{kd_1}\left[1-\frac{\epsilon_A}{\epsilon_B}\right]+A_-e^{-kd_1}\left[1+\frac{\epsilon_A}{\epsilon_B}\right]\right], \tag{26}$$

$$B'_+=\frac{1}{2}\left[A'_+e^{kd_1}\left[1+\frac{\epsilon_A}{\epsilon_B}\right]+A'_-e^{-kd_1}\left[1-\frac{\epsilon_A}{\epsilon_B}\right]\right], \tag{27}$$

$$B'_-=\frac{1}{2}\left[A'_+e^{kd_1}\left[1-\frac{\epsilon_A}{\epsilon_B}\right]+A'_-e^{-kd_1}\left[1+\frac{\epsilon_A}{\epsilon_B}\right]\right]. \tag{28}$$

Substituting (25) and (26) into (19) and (20), respectively, we obtain

$$A_++A_-=e^{\gamma L}\left\{\frac{1}{2}\left[A_+e^{kd_1}\left[1+\frac{\epsilon_A}{\epsilon_B}\right]+A_-e^{-kd_1}\left[1-\frac{\epsilon_A}{\epsilon_B}\right]\right]e^{kd_2}+\frac{1}{2}\left[A_+e^{kd_1}\left[1-\frac{\epsilon_A}{\epsilon_B}\right]+A_-e^{-kd_1}\left[1+\frac{\epsilon_A}{\epsilon_B}\right]\right]e^{-kd_2}\right\} \tag{29}$$

and

$$\frac{\epsilon_A}{\epsilon_B}(A_+-A_-)=e^{\gamma L}\left\{\frac{1}{2}\left[A_+e^{kd_1}\left[1+\frac{\epsilon_A}{\epsilon_B}\right]+A_-e^{-kd_1}\left[1-\frac{\epsilon_A}{\epsilon_B}\right]\right]e^{kd_2}-\frac{1}{2}\left[A_+e^{kd_1}\left[1-\frac{\epsilon_A}{\epsilon_B}\right]+A_-e^{-kd_1}\left[1+\frac{\epsilon_A}{\epsilon_B}\right]\right]e^{-kd_2}\right\}, \tag{30}$$

where we have dropped the functional dependence of ϵ for brevity. Adding and subtracting (29) and (30) yields the following matrix equation:

$$\begin{bmatrix}\left[1+\frac{\epsilon_A}{\epsilon_B}\right](e^{kd_1}-e^{-\gamma L}e^{-kd_2}) & \left[1-\frac{\epsilon_A}{\epsilon_B}\right](e^{-kd_1}-e^{-\gamma L}e^{-kd_2})\\ \left[1-\frac{\epsilon_A}{\epsilon_B}\right](e^{kd_1}-e^{-\gamma L}e^{kd_2}) & \left[1+\frac{\epsilon_A}{\epsilon_B}\right](e^{-kd_1}-e^{-\gamma L}e^{kd_2})\end{bmatrix}\begin{bmatrix}A_+\\A_-\end{bmatrix}=\begin{bmatrix}0\\0\end{bmatrix}. \tag{31}$$

Similarly, by substituting (27) and (28) into (23) and (24), and then adding and subtracting the resulting equations, we find

$$\begin{bmatrix}\left[1+\frac{\epsilon_A}{\epsilon_B}\right](e^{kd_1}-e^{\gamma L}e^{-kd_2}) & \left[1-\frac{\epsilon_A}{\epsilon_B}\right](e^{-kd_1}-e^{\gamma L}e^{-kd_2})\\ \left[1-\frac{\epsilon_A}{\epsilon_B}\right](e^{kd_1}-e^{\gamma L}e^{kd_2}) & \left[1+\frac{\epsilon_A}{\epsilon_B}\right](e^{-kd_1}-e^{\gamma L}e^{-kd_2})\end{bmatrix}\begin{bmatrix}A'_+\\A'_-\end{bmatrix}=\begin{bmatrix}0\\0\end{bmatrix}. \tag{32}$$

Setting the determinant of the coefficient matrix equal to zero in both (31) and (32) yields the same condition on γ, as follows:

$$\cosh(\gamma L)=\cosh(kd_2)\cosh(kd_1)+1/2\left[\frac{\epsilon_B}{\epsilon_A}+\frac{\epsilon_A}{\epsilon_B}\right]\sinh(kd_2)\sinh(kd_1). \tag{33}$$

Note that this implicit dispersion relation for γ is identical to Eq. (14) with $i\gamma$ substituted for q.

Next, we impose the boundary conditions at the C-A interface, $z=0$, to obtain

$$C=A_++A_-+A'_++A'_- \tag{34}$$

and

$$\epsilon_C(\omega)C=\epsilon_A(\omega)(A_+-A_-+A'_+-A'_-). \tag{35}$$

Imposing the boundary conditions at the B-D interface, $z=pL$, results in

$$De^{-kpL}=e^{-\gamma pL}e^{\gamma L}(B_+e^{kd_2}+B_-e^{-kd_2})+e^{\gamma pL}e^{-\gamma L}(B'_+e^{kd_2}+B'_-e^{-kd_2}), \tag{36}$$

$$-\epsilon_D(\omega)De^{-kpL}=\epsilon_B(\omega)[e^{-\gamma pL}e^{\gamma L}(B_+e^{kd_2}-B_-e^{-kd_2})+e^{\gamma pL}e^{-\gamma L}(B'_+e^{kd_2}-B'_-e^{-kd_2})]. \tag{37}$$

By substituting Eq. (19) and (23) into (36) we obtain

$$De^{-kpL}=e^{-\gamma pL}(A_+ +A_-)+e^{\gamma pL}(A'_+ +A'_-)\ , \quad (38)$$

and doing the same with (20), (24), and (37) results in

$$-\epsilon_D(\omega)De^{-kpL}=\epsilon_A(\omega)[e^{-\gamma pL}(A_+ -A_-) +e^{\gamma pL}(A'_+ -A'_-)]\ . \quad (39)$$

We now solve for A_- in terms of A_+. From Eqs. (31) and (32) we find

$$A_- =KA_+\ , \quad (40)$$

$$A'_- =K'A'_+\ , \quad (41)$$

where

$$K=-\frac{[1+(\epsilon_A/\epsilon_B)](e^{kd_1}-e^{-\gamma L}e^{-kd_2})}{[1-(\epsilon_A/\epsilon_B)](e^{-kd_1}-e^{-\gamma L}e^{-kd_2})} \quad (42)$$

and

$$K'=-\frac{[1+(\epsilon_A/\epsilon_B)](e^{kd_1}-e^{+\gamma L}e^{-kd_2})}{[1-(\epsilon_A/\epsilon_B)](e^{-kd_1}-e^{+\gamma L}e^{-kd_2})}\ . \quad (43)$$

Finally, by substituting (40) and (41) into Eqs. (34), (35), (38), and (39) we obtain

$$\begin{bmatrix} 1+K & 1+K' & -1 & 0 \\ \epsilon_A(1-K) & \epsilon_A(1-K') & -\epsilon_C & 0 \\ e^{-\gamma pL}(1+K) & e^{\gamma pL}(1+K') & 0 & -e^{-kpL} \\ \epsilon_A e^{-\gamma pL}(1-K) & \epsilon_A e^{\gamma pL}(1-K') & 0 & \epsilon_D e^{-kpL} \end{bmatrix} \begin{bmatrix} A_+ \\ A'_+ \\ C \\ D \end{bmatrix} = \begin{bmatrix} 0 \\ 0 \\ 0 \\ 0 \end{bmatrix}\ . \quad (44)$$

The above system of equations admits a solution only if the determinant of the coefficient matrix vanishes. This leaves us, after some algebra, with the following result:

$$[\epsilon_A^2(1-K)(1-K')-\epsilon_C\epsilon_D(1+K)(1+K')-\epsilon_A\epsilon_C(1-KK')+\epsilon_A\epsilon_D(1-KK')]\tanh(\gamma pL)-\epsilon_A(\epsilon_C+\epsilon_D)(K-K')=0\ . \quad (45)$$

Equation (41) is the implicit dispersion relation for the finite superlattice. We note that this equation is particularly convenient since the number of layers in the finite superlattice, p, appears only in the argument of the hyperbolic tangent function. This makes numerical calculations relatively easy.

III. NUMERICAL EXAMPLES OF DISPERSION RELATIONS

In this section we present numerical examples for the dispersion relations. As has been pointed out earlier, the theoretical results derived in the preceding section describe collective excitations which can arise from many different microscopic mechanisms. It is only necessary to know the frequency-dependent dielectric constants of the various materials involved. For the examples considered here, we have chosen a rather simple model system of metal slabs separated by dielectric layers. The simplicity of the system allows us to understand general trends quite easily. For these applications, we assume the dielectric constant of material A is given by $\epsilon_A(\omega)=1-\omega_P^2/\omega^2$. We take $\omega_P=15$ eV, which is appropriate for Al. We further suppose that the dielectric gaps have frequency-independent dielectric constants.

We now want to answer the two questions posed earlier:

(1) How many layers of a superlattice are required before one can approximate the finite superlattice by an infinite (for bulk modes) or semi-infinite (for surface modes) superlattice?

(2) Are there any unique features to be found only in the finite superlattice? We will answer these questions by the examples presented below.

Figure 2 presents the dispersion curves for a superlattice composed of twenty films of Al, surrounded by materials such that $\epsilon_B=\epsilon_C=\epsilon_D=1$. The boundaries of the bulk bands, as well as the frequency of the surface modes, agree very nearly with those values found for the semi-infinite superlattice with the same parameters. Basically, the continuous band of states found in the infinite or semi-infinite superlattice breaks up into closely spaced

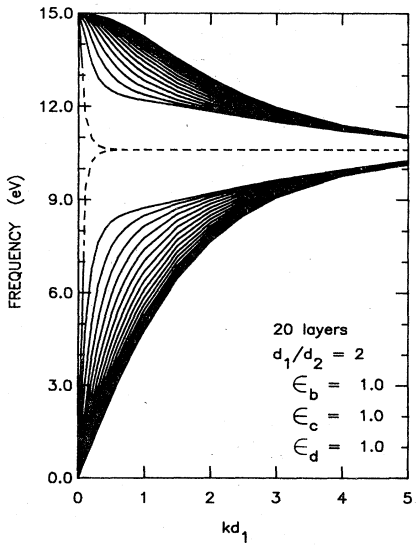

FIG. 2. Dispersion curves for the case where material A is aluminum, materials B, C, and D are vacuum, and there are twenty layers of material A. Note the discrete allowed modes and splitting of the surface modes, as discussed in the text.

discrete states in the finite-sized superlattice. Thus the dispersion curve for the twenty-layer case is a reasonable approximation to the semi-infinite superlattice results. One significant exception to this is in the region $kd_1 < 0.3$. In this region the wavelength of the plasmon is large compared to the thickness of a film and can also be large compared to the thickness of the superlattice. As a result, a surface plasmon at the top surface of the superlattice can interact with a surface plasmon at the bottom of the superlattice. This interaction produces the splitting of the surface-plasmon frequency which is visible in Fig. 2. A similar situation occurs in properties of surface plasmons on a *single* film. As the thickness is reduced, the surface plasmons at the top and bottom interact, with a net result that there are two surface-plasmon frequencies.

One further difference between the semi-infinite and finite cases considered here is that the surface modes actually merge continuously into a bulk mode. This is more easily seen in Fig. 3, which presents the dispersion curves for ten films of Al. Here we see that at $kd_1 = 0.2$ the surface mode changes in character to a bulk mode for the lower band. We also note that the splitting of the surface modes also occurs at a much larger value of kd_1 when comparing Fig. 3 to Fig. 2. Again, we see that as the thickness of the superlattice becomes close to the wavelength of the surface plasmon, the splitting becomes visible.

We note that in Fig. 3 the boundaries of the bulk bands are still very close to the values found in the semi-infinite case. If we continue to reduce the number of Al layers, the frequency region of the bulk modes finally deviates significantly from that of the infinite case. In Fig. 4 we present the case where the number of Al films is just five. A comparison of Figs. 2 and 4 indicates that the deviation can be quite significant.

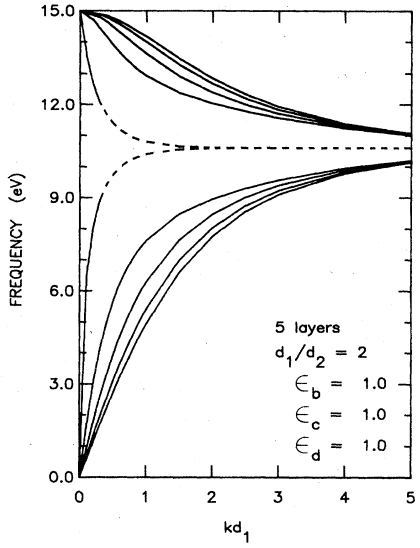

FIG. 4. Collective-mode frequencies for a superlattice consisting of five layers of material A, $\epsilon_B, \epsilon_C, \epsilon_D = 1$. Material A is aluminum. The frequencies of the bulk bands differ from Fig. 3 and a surface-mode split exists to $kd_1 \cong 1.5$.

For the semi-infinite structure, it was shown that plots of frequency versus the ratio d_1/d_2 also give very interesting information. The ratio d_1/d_2 is easily altered experimentally, and thus is an important parameter in the characterization of a superlattice. For the semi-infinite case, one sees in such a plot two bulk bands. These bands are always separated by a gap, except at $d_1 = d_2$. Also it was seen that the surface mode was only allowed in the region where $d_1 > d_2$. In Fig. 5 we present the equivalent set of curves as those described above, but now for the finite superlattice. We see several significant differences.

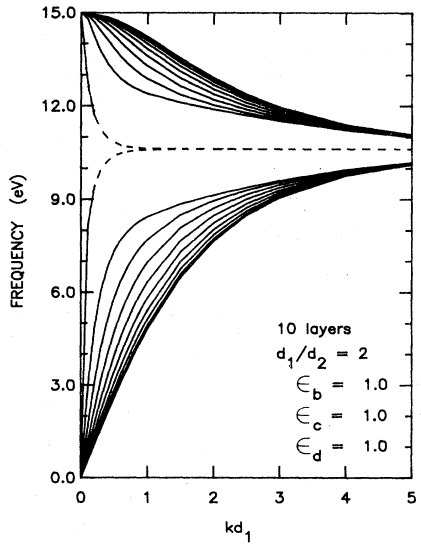

FIG. 3. Dispersion curves for the same material parameters as Fig. 2, except there are ten layers of material A. The bulk-mode boundaries are similar to those of Fig. 2. The surface-mode split is visible for larger values of kd_1.

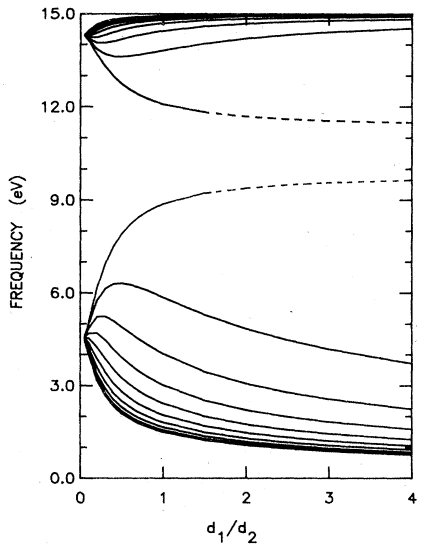

FIG. 5. For a ten-layer superlattice, $\epsilon_B = \epsilon_C = \epsilon_D = 1$, we show the allowed frequencies as a function of d_1/d_2 with $kd_1 = 0.2$. Note the complete separation of bulk bands, as described in the text.

First, the two bulk bands remain completely separate for all values of the ratio d_1/d_2. Secondly, the surface modes now emerge from a particular bulk mode and there are two surface modes as discussed before.

We now turn to a more realistic case where material B is an insulating spacer, and the layered films are resting on an insulating substrate. We consider a structure where $\epsilon_B=3.0$, $\epsilon_C=1.0$, and $\epsilon_D=2.5$. These values are appropriate for the case where material B is Al_2O_3 and the substrate is SiO_2. In addition, we have chosen $d_1/d_2=2$. The dispersion curves for the bulk and surface modes in this case are presented in Fig. 6. The most striking feature in this set of curves is a short segment of surface mode which emerges from an upper-bulk-mode branch and exists as a surface mode in the region $0.5<kd_1<1.3$ and then becomes a bulk mode again. In this region, the dispersion curve is nearly flat.

We would like to note several other features visible in Fig. 6: (1) There is a surface mode for large kd_1 at a frequency of 10.6 eV. This frequency corresponds to that of a surface mode at the interface of Al and vacuum in a semi-infinite geometry. (2) If we compare the frequency of the bulk and surface modes in Fig. 6 with those in Fig. 3, we see that they are generally down-shifted. This is caused by the screening of the metal layers from each other by the intervening dielectric slabs. (3) There is a second surface mode at lower frequencies that exists for all values of kd_1. The frequency of this mode is nearly independent of the wave vector (7.8 eV). In the next section we will see that this mode is localized at the last metal-insulator interface before the substrate.

Figure 7 illustrates the case where the thickness ratio is inverted, i.e., $d_1/d_2=0.5$ rather than 2 as in Fig. 6. We see in this figure that the frequencies are further down-shifted when compared to Fig. 6. This is because the increase in the insulator thickness further isolates the metal films. Note that in this figure the bulk modes are considerably more compressed in comparison to the preceding figure. This results because the large gaps between metal films reduces the coupling strengths between the surface excitations on each metal film, which in turn reduces the bandwidth of the bulk excitations, a result similar to the reduction in bandwidth for electronic states when the atoms are moved further apart. It is also interesting to note that the surface mode seen in Fig. 6, which existed only in a short range of values of kd_1, is no longer present.

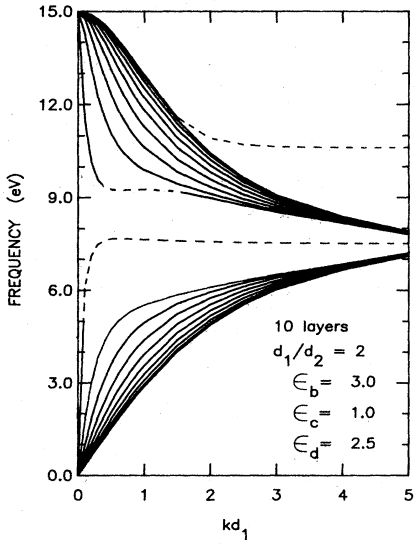

FIG. 6. For the physically realistic case $\epsilon_B=3$ (Al_2O_3), $\epsilon_D=2.5$ (SiO_2), $\epsilon_C=1$, we show the collective-mode frequencies for a ten-layer structure. Material A is aluminum. The bottom surface produces a characteristic mode at $\omega\cong 7.8$ eV.

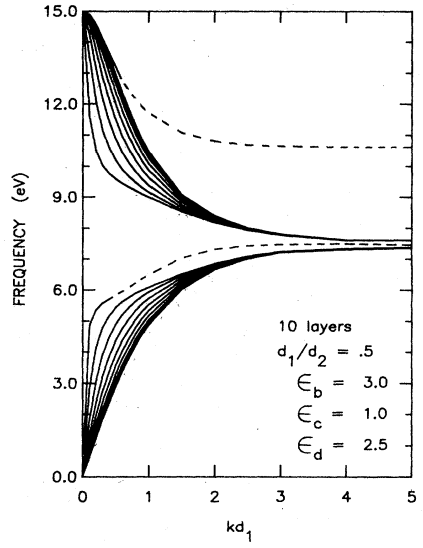

FIG. 7. Collective-mode spectrum for a ten-layer superlattice, $\epsilon_B=3$, $\epsilon_D=2.5$, $\epsilon_C=1$, material A is aluminum, with $d_1=\frac{1}{2}d_2$.

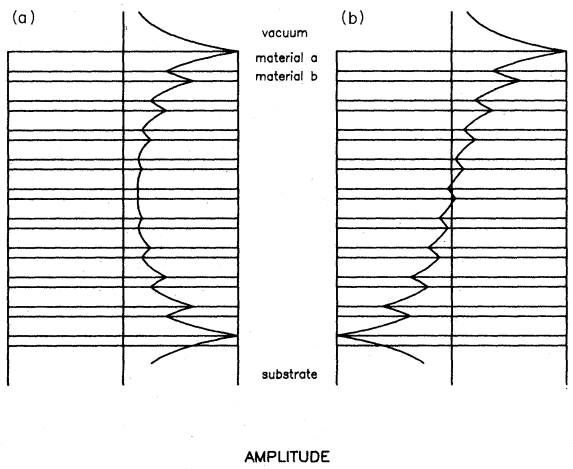

FIG. 8. The electrostatic potential as a function of depth for a ten-layer superlattice, $\epsilon_B=\epsilon_C=\epsilon_D=1$. These are the potentials for the surface mode of Fig. 3 where $kd_1=1$ and in (a) $\omega=10.59$ eV and in (b) $\omega=10.62$ eV.

IV. ELECTROSTATIC POTENTIALS

In the preceding section we demonstrated that in finite superlattices there exists a discreet number of allowed plasmon modes. Furthermore, we demonstrated the splitting of surface modes and the emergence of surface-mode pairs unique to finite structures. In this section we present numerical studies of the electrostatic potential as a function of depth into the superlattice. These are interesting because they show the physical nature of the collective modes, that is, they give the location of strong localizations, etc. In what follows we suppose a superlattice consisting of ten layers of aluminum films separated by a dielectric gap, the whole resting on a dielectric substrate.

Figure 8 shows the potential curves for the case where $\epsilon_B=\epsilon_C=\epsilon_D=1$, $kd_1=1$ and (a) $\omega=10.59$ and (b) 10.622. This corresponds to the region in dispersion curve Fig. 3 where the surface-mode splitting becomes substantial.

As briefly discussed in the preceding section, the appearance of split surface-mode frequencies in a finite superlattice is analogous to the splitting of frequencies on a single film. For an isolated film each surface can support a mode. These modes couple to produce an odd-parity and an even-parity pair, split by interaction between the two surfaces. Because the structure depicted in Fig. 8 is symmetric about the midplane, the long-wavelength surface modes must couple into an odd-even—parity pair as well.

Figure 9 shows examples of bulk excitations, again for the symmetric structure where $\epsilon_B=\epsilon_C=\epsilon_D=1$. In (a) $\omega_-=8.45$ and in (b) $\omega_+=12.39$. These correspond to the uppermost ω_- mode and the lowermost ω_+ mode, respectively, in Fig. 3. It must be noted that while these are indeed bulk modes of the superlattice as a whole, they are composed of coupled surface plasmons which reside at the material interfaces.

For a finite superlattice, it is interesting to consider the effects of small perturbations on the collective modes. Figure 10 demonstrates the effect of a 5% increase in the dielectric constant of the gaps on the surface-mode

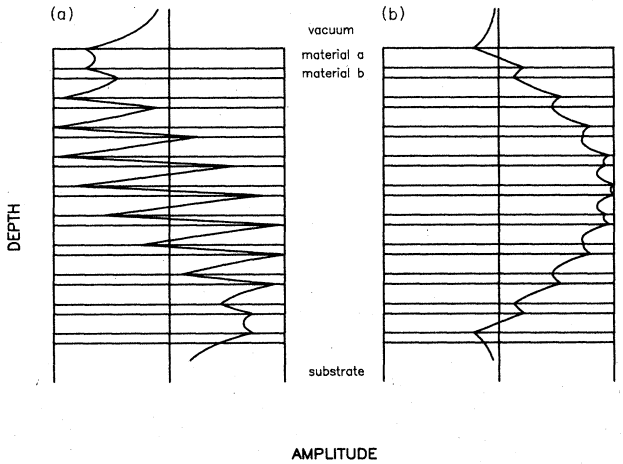

FIG. 9. Potential curves for bulk modes with the same geometry and materials as in Fig. 8. Here $kd_1=1.0$ and in (a) $\omega=8.45$ eV and in (b) $\omega=12.39$ eV.

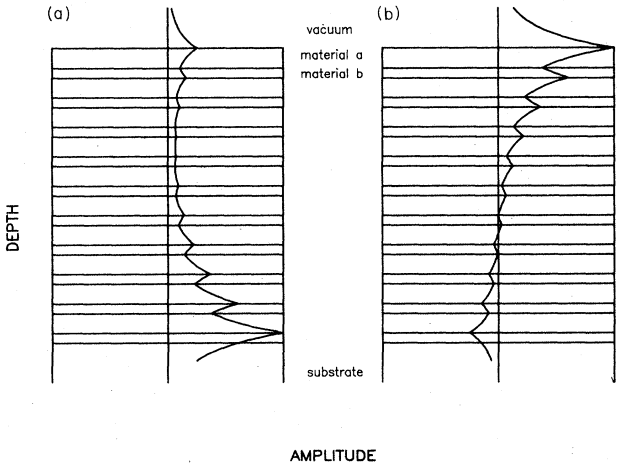

FIG. 10. Potential curves for the two surfaces modes as in Fig. 8, except that the dielectric constant of material B has been increased by 5%. Again $kd_1=1.0$ and the frequencies are now (a) $\omega=10.51$ eV and (b) $\omega=10.57$ eV. Note that the small change in dielectric constant strongly localizes the surface modes.

behavior ($\epsilon_B=1.05$ and $\epsilon_C=\epsilon_D=1$). It should be noted that this increase does not affect the dispersion curves appreciably (less than 5% change), but serves to strongly localize the surface-mode pair, as can clearly be seen by comparison of Figs. 8 and 10. The slight lowering of symmetry dramatically uncouples the pair, leaving two modes, each of which is supported at a different surface.

The final three figures all represent the physically realistic case discussed previously: ten aluminum films separated by films of Al_2O_3, the entire structure resting on an SiO_2 substrate ($\epsilon_B=3$, $\epsilon_D=2.5$, $\epsilon_C=1$). We recall that a unique feature of this dispersion curve was the emergence of a short segment of surface mode emerging at

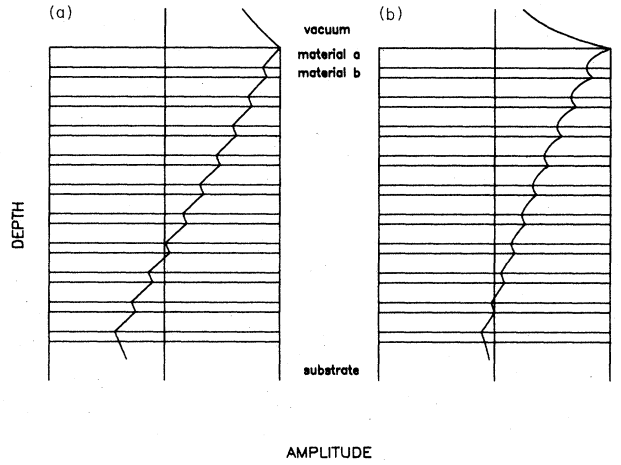

FIG. 11. The evolution of the surface mode seen in Fig. 6. We show the potentials for (a) $kd_1=0.2$ and $\omega=10.145$ eV, and (b) $kd_1=0.7$ and $\omega=9.24$ eV. Note the change in character from bulk to surface as kd_1 increases.

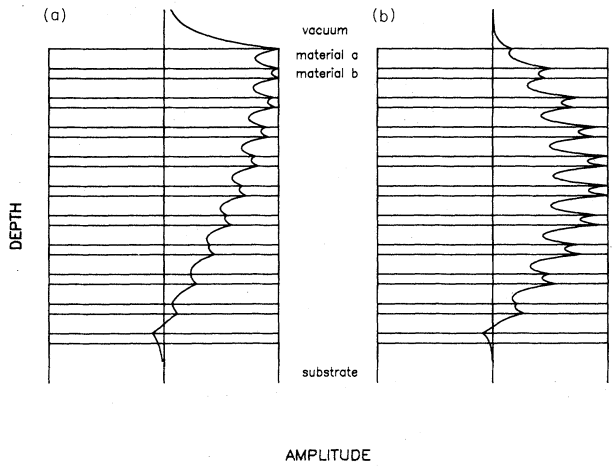

FIG. 12. Continuation of the surface-mode evolution from Fig. 6. In (a) $kd_1=1.4$ and $\omega=9.23$ eV, in (b) $kd_1=2.5$ and $\omega=8.75$ eV. Case (b) clearly shows bulk character even though it is still localized near the upper boundary.

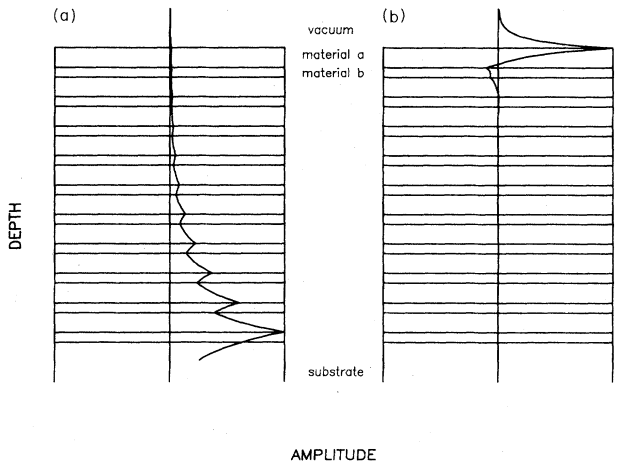

FIG. 13. Potential curves for the upper and lower surface modes seen in Fig. 6. In (a) $kd_1=1.0$ and $\omega=7.64$ eV. In (b) $kd_1=3.0$ and $\omega=10.67$ eV. These modes are clearly localized at opposite surfaces of the superlattice.

long wavelengths from the bulk bands, and the presence of a new surface mode between the bulk bands. Figures 11 and 12 illustrate the evolution of the short surface mode from the bulk bands. Figure 11 shows the mode in the extreme long-wavelength region [kd=(a) 0.2, (b) 0.70]. Even in this region, the branch appears strongly localized at the upper surface of the superlattice. As we trace into the shorter wavelengths, Fig. 12 [kd= (a) 1.4, (b) 2.5], the bulk character of the mode becomes evident; however, the largest amplitude remains in the upper portion of the structure.

Figure 13(a) is the potential for the surface mode which emerges from the upper bulk band of Fig. 6 and exists at $\omega=10.67$ eV for all large kd_1. The fact that the potential resides almost entirely within the top film, and decays to zero everywhere else, shows that it will remain at 10.6 eV regardless of the dielectric parameters or the number of layers. Thus this mode corresponds to a simple surface mode on a semi-infinite aluminum substrate.

The low-frequency surface mode, which exists for all kd_1, is a characteristic of finite superlattices. This mode does not exist in semi-infinite structures. The introduction of a bottom surface also introduces another surface mode, and indeed Fig. 13(a) demonstrates that this mode is strongly localized at the bottom Al-Al_2O_3 interface.

V. SUMMARY

We have derived the general dispersion relations for a superlattice of finite extent, applicable to any choice of material parameters and any number of films. Through numerical examples utilizing aluminum films separated by dielectric gaps, we showed that twenty layers of two materials reflected the results for a semi-infinite structure, and that ten layers also showed reasonable similarity to the semi-infinite results with the exception of an appreciable splitting of the surface mode into an odd- and even-parity pair. It was also shown that a small change in the dielectric constant of the spacers significantly localized the surface modes, one supported at each boundary of the superlattice. The physically realistic case, consisting of ten aluminum films separated by Al_2O_3 dielectric spacers with the entire structure resting on a SiO_2 substrate, demonstrated the characteristic down-shift in frequency provided by the dielectric constant of the Al_2O_3. In this structure, we also showed the existence of a surface mode not present in the semi-infinite structure. It was demonstrated by examining the electrostatic potential as a function of depth that this new mode is localized at the bottom of the superlattice.

ACKNOWLEDGMENT

We want to thank the University of Colorado, Colorado Springs for support of this work and for partial support of one of us (B. L. J.).

[1]Yu A. Bespjatyich, A. W. Varhkovskij, W. J. Subkov, and H. Pfeifer, Fiz. Tverd. Tela (Leningrad) **19**, 1743 (1977) [Sov. Phys.—Solid State **19**, 1017 (1977)].

[2]R. E. Camley, Talat S. Rahman, and D. L. Mills, Phys. Rev. B **27**, 261 (1983).

[3]P. Grunberg and K. Mika, Phys. Rev. B **27**, 2955 (1983).

[4]M. Grimsditch, M. R. Khan, A. Kueny, and I. K. Schuller, Phys. Rev. Lett. **51**, 498 (1983).

[5]R. Krishnan, W. Jantz, W. Wettling, and G. Rupp, IEEE Trans. Magn. **MAG-20**, 1264 (1984).

[6]G. Rupp, W. Wettling, and W. Jantz, Appl. Phys. (to be published).

[7]B. A. Auld, G. S. Beaupre, and G. Gerrmann, Electron Lett. **13**, 525 (1977).

[8]R. E. Camley, B. Djafari-Rouhani, L. Dobrzynski, and A. A. Maradudin, Phys. Rev. B **27**, 7318 (1983).

[9]B. Djafari-Rouhani, L. Dobrzynski, O. Hardouin Duparc, R. E. Camley, and A. A. Maradudin, Phys. Rev. B **28**, 1711 (1983).
[10]M. V. Klein, C. Colvard, R. Fischer, and H. Morkoç, J. Phys. (Paris) Colloq. **45**, C5-131 (1984).
[11]J. Sapriel, J. C. Michel, J. C. Toledano, and R. Vacher, J. Phys. (Paris) Colloq. **45**, C5-139 (1984).
[12]B. Jusserand, D. Paquet, J. Kervarec, and A. Regreny, J. Phys. (Paris) Colloq. **45**, C5-139 (1984).
[13]V. Narayanamurti, J. Phys. (Paris) Colloq. **45**, C5-157 (1984).
[14]A. Kueny and M. Grimsditch, Phys. Rev. B **26**, 4699 (1982).
[15]A. L. Fetter, Ann. Phys. (N.Y.) **88**, 1 (1974).
[16]R. E. Camley and D. L. Mills, Phys. Rev. B **29**, 1695 (1984).
[17]G. F. Giuliani and J. J. Quinn, Phys. Rev. Lett. **51**, 919 (1983).
[18]A. C. Tselis and J. J. Quinn, Phys. Rev. B **29**, 3318 (1984).
[19]W. L. Bloss, J. Vac. Sci. Technol. B **1**, 431 (1983).
[20]D. Olego, A. Pinczuk, A. C. Gossard, and W. Wiegmann, Phys. Rev. B **25**, 7867 (1982).
[21]Jainendra K. Jain and Phillip B. Allen, Phys. Rev. Lett. **54**, 947 (1985).
[22]G. S. Agarwal, Phys. Rev. B **31**, 3534 (1985).